PHYSICAL REVIEW B **70**, 235420 (2004)

Chemical effects at the buried NiO/Fe(001) interface

M. Finazzi,* A. Brambilla, L. Duò, G. Ghiringhelli, M. Portalupi, and F. Ciccacci
INFM - Dipartimento di Fisica del Politecnico di Milano, Piazza L. da Vinci 32, 20133 Milano, Italy

M. Zacchigna and M. Zangrando
INFM - TASC, Basovizza S.S. 14, Km 163.5, 34012 Trieste, Italy

(Received 11 November 2003; revised manuscript received 21 June 2004; published 23 December 2004)

X-ray absorption spectroscopy and x-ray magnetic circular dichroism have been applied to study the oxidation reactions at the buried interface resulting from NiO deposition on Fe(001). The NiO layer is obtained by reactive deposition; i.e., by evaporating Ni in an O_2 atmosphere. We find that NiO reactive deposition on Fe(001) promotes Fe oxidation, leading to the formation of a thick, oxygen-rich oxide, identified as Fe_3O_4. This ferrimagnetic interface oxide shows a net magnetization that couples ferromagnetically to the iron substrate. This behavior is different from the case of the Fe/NiO(001) interface, where formation of (antiferromagnetic) FeO occurs. A sample annealing following the growth of the NiO/Fe interface is found to reduce the iron and to induce Ni diffusion in the Fe substrate.

DOI: 10.1103/PhysRevB.70.235420 PACS number(s): 81.65.Mq, 75.70.−i

I. INTRODUCTION

The characterization of the oxidation/reduction chemical reactions and interdiffusion at the interface between a ferromagnetic (FM) metal and an antiferromagnetic (AFM) oxide is a key issue to understand the electronic and magnetic properties of such interfaces. Among these properties, let us mention the exchange bias effect, consisting in the breaking of time reversal symmetry and the onset of unidirectional magnetic anisotropy in a field-cooled FM/AFM interface.[1] The structural and chemical properties of the AFM/FM interface is crucial to determine the type of coupling between the FM and AFM anisotropy axes[2,3] as well as the density of AFM uncompensated moments and magnitude of the exchange bias effect.[4–6]

Among AFM/FM systems, the NiO/Fe interface has attracted considerable attention[7–11] because of the high NiO Néel temperature ($T_N = 520$ K), and the low lattice mismatch between Fe and NiO. In particular, it has been observed that, when Fe is deposited on the NiO(001) surface, partial oxidation/reduction of one or two atomic layers occurs on either side of the interface.[12] Considering the potential applications of such studies to the preparation of tunneling magnetoresistance junctions, where both types of interfaces (FM/AFM and FM/AFM) would be present in the same device, it is worth investigating whether and to which extent the growth sequence (i.e., AFM/FM versus FM/AFM) is relevant. *A priori*, it could be considered that the two kinds of interface are the same. This naive picture has recently been dismissed by the evidence that in the case of NiO/Fe(001), the magnetic moments of the Ni atoms are oriented in-plane and perpendicular to the magnetization of the Fe substrate,[10] at variance with the Fe/NiO(001) case, in which the Fe and Ni moments tend to be collinear.[5,8,9] This can be accounted for by a micromagnetic model showing a tradeoff between the two relative orientations depending both on the amount of uncompensated moments at the interface and on the interface exchange field.[3] Besides showing differences concerning magnetic aspects, the two systems may also differ in the dynamics of the oxidation/reduction chemical processes occurring at the metal/oxide buried interface during the growth of the overlayer.

To tackle this problem, hereafter we report about the redox reactions occurring at the NiO/Fe(001) interface, obtained by deposition of nickel on a Fe(001) substrate in an oxygen atmosphere (a technique known as reactive deposition). The chemical composition at the interface is studied by applying x-ray absorption spectroscopy (XAS) and x-ray magnetic circular dichroism (XMCD). We find that the oxidation/reduction chemical processes occurring at the NiO/Fe interface strongly depend on the growth sequence. When iron is grown on NiO(001), formation of a few atomic layers of FeO is promoted,[12] while we show here that depositing NiO on Fe(001) results in the creation of an oxygen-rich iron oxide. A thermal treatment after the (room temperature) growth makes oxygen desorb and Ni dissolve into the Fe lattice, with formation of FeO at the topmost layers of the system.

II. EXPERIMENT

High quality epitaxial NiO films can be prepared by reactive deposition, evaporating Ni from a high purity rod in a 8×10^{-7} mbar O_2 atmosphere on a Fe(001) substrate kept at room temperature.[11] In the present work, we investigate the redox reactions occurring when the NiO film has a thickness equal to 20 atomic layers (ML). The NiO thickness was determined by first calibrating the Ni evaporation rate with a quartz microbalance before letting oxygen into the preparation chamber. We then established how long to open the shutter of the Ni evaporator in O_2 atmosphere to deposit the amount of Ni atoms per unit surface corresponding to the desired NiO thickness.

The Fe(001) substrate was a thick Fe film ($\geqslant 3000$ Å) on MgO(001), whose surface was cleaned *in situ* by cycles of Ar sputtering and annealing at 850 K. Since in the first stages of reactive Ni deposition the iron substrate is necessarily exposed to oxygen, for the sake of reliability and reproducibility we decided to first passivate the Fe(001) surface. For this reason, we annealed the clean Fe(001) substrate in an O_2 atmosphere obtaining the well characterized and stable Fe(001)-$p(1\times 1)$O surface.[13,14] Note that such a passivated surface is very stable to further oxidation. In the following, for simplicity, the NiO film grown on such a substrate will be addressed simply as NiO/Fe(001). The high-surface-sensitive inverse photoemission data reported in Ref. 11 demonstrate that such NiO/Fe(001) layers thicker are certainly continuous for a film thickness above 10 ML since a signal from iron is no longer detected.

Light-polarization-dependent spectra were collected in the total electron yield (TEY) mode by measuring the sample drain current at the beamline BACH at ELETTRA,[15] the Italian synchrotron radiation facility in Trieste. In particular, the XMCD data were measured reversing the circular light polarization, while the iron substrate magnetization was kept constant and in-plane. The angle between the sample normal and the direction of light propagation was 60°. The XAS signal has been obtained by averaging the two spectra collected with opposite circular light polarization. XAS and XMCD combine the site sensitivity typical of a core level spectroscopy to a large probing depth, both being essential to investigate the chemical composition of the buried interface covered by a 20 ML thick NiO layer. For reference, the XAS and XMCD spectra of the $NiFe_2O_4$ ferrite, measured at the ID12B beamline at the European Synchrotron Radiation Facility in Grenoble, are also given.

III. RESULTS AND DISCUSSION

The XAS and XMCD signals at the Fe $L_{2,3}$ edge obtained from Fe(001)-$p(1\times 1)$O and 20 ML NiO/Fe(001) are displayed in Fig. 1. Both the XAS and XMCD spectra from the Fe(001)-$p(1\times 1)$O substrate are very similar to the ones reported in the literature for a clean Fe surface.[16] This is not surprising, in view of the large probing depth of x-ray absorption spectroscopy in the TEY mode compared to one atomic layer of oxide that forms at the Fe(001)-$p(1\times 1)$O surface. A value of 15 Å has been reported for the escape depth of secondary electrons in iron.[16] The spectra obtained on 20 ML NiO/Fe(001) show clear fingerprints of oxidation of the Fe substrate, visible as an atomic multiplet fine structure on both the XAS and XMCD signals and indicating a localization of the electron states. Because of the large probing depth, the substrate contribution to the 20 ML NiO/Fe(001) XAS and XMCD spectra at the Fe $L_{2,3}$ edge is considerable. In Fig. 1 we show the spectra of the oxide layer obtained by subtracting the substrate contribution as estimated mainly by the XMCD spectrum, following the same procedure described in Ref. 17. Figure 1 compares the difference spectra with the XAS and XMCD obtained from bulk Fe_3O_4 and $NiFe_2O_4$, which are ferrimagnetic.[17,18] In all cases, the XMCD data show qualitatively similar profiles, with two negative peaks (at about 708 and 710 eV, respectively) and a positive one in between.

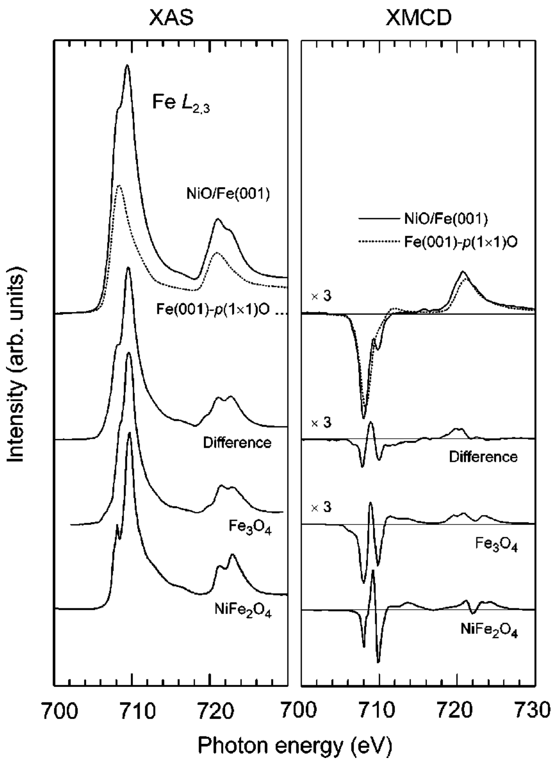

FIG. 1. Comparison between the Fe $L_{2,3}$ XAS (left) and XMCD (right) spectra from 20 ML NiO/Fe(001) and Fe(001)-$p(1\times 1)$O. After normalization, the spectra obtained on Fe(001)-$p(1\times 1)$O have been multiplied by a factor equal to 0.5. The difference spectra are compared to the Fe_3O_4 (from Ref. 17) and to the $NiFe_2O_4$ XAS and XMCD.

During the NiO film growth, substrate Fe atoms can interact with both O and Ni atoms. For example, in the case of the Fe/NiO(001) interface this causes, beside the formation of FeO, the appearance of some Fe-Ni intermixing at the interface.[19] Looking more closely at the XMCD spectra it can be seen that, while both for the difference spectrum and the Fe_3O_4 profile the low energy negative peak is quite larger than the high energy one (with an intensity ratio of about 1.4), for the $NiFe_2O_4$ ferrite the situation is opposite (with an intensity ratio of about 0.7), indicating that the XMCD fine structure is sensitive to the chemical environment. This different behavior is mainly related to the Fe ion valence:[18] Fe_3O_4 is characterized by the simultaneous presence of Fe^{2+} (33.3%) and Fe^{3+} (66.6%) sites, whereas in $NiFe_2O_4$ iron has only Fe^{3+} sites. Similar XMCD results are obtained for other ferrites (e.g.,. in Ref. 18 for $CoFe_2O_4$), which has the same valence structure. Even considering the small uncertainty in the estimation of the substrate contribution, the strong similarities between the difference and the Fe_3O_4 XAS and XMCD spectra over the entire energy range clearly indicate that Fe_3O_4 formation occurs at the interface with no sizeable Fe-Ni mixing within the oxide film.

Reactive deposition of Ni on Fe(001)-$p(1\times 1)$O leads to very similar results, in terms of iron oxidation state, as does room temperature Fe exposure to O_2, which leads to the formation of Fe_3O_4 as well.[12,17,20] A general result in fact is that Fe_3O_4 is formed when oxygen is available in large quantities. However, an important difference is that the Fe_3O_4 formed after exposure of iron to O_2 is coupled antiferromagnetically to the underlying metal;[17] i.e., the sign of the Fe_3O_4 XMCD spectrum is inverted with respect to that of bulk Fe_3O_4.[21] On the contrary, in our data we observe a ferromagnetic coupling between the substrate and the oxide. This implies that the energetics of a Fe_3O_4 film magnetically coupled with an iron substrate by the exchange interaction is dramatically altered by the presence of an AFM NiO overlayer. Note also that, although the shape of the difference and Fe_3O_4 XMCD spectra are in good agreement, the magnitude of the dichroism in the difference is about a factor of 2 smaller than the one measured on bulk Fe_3O_4,[17,21] indicating a loss of magnetization in the interface oxide.

Our analysis clearly shows that the type of iron oxide forming at the Fe/NiO interface depends on the growth sequence. In fact, the interface oxide that results when Fe is deposited on NiO has been identified with FeO, which is antiferromagnetic. The different oxidation and magnetic state of the interface oxide might have important consequences in determining the different magnetic properties observed in Fe/NiO(001) and in the reverse NiO/Fe(001) interface,[10] with possible effects on exchange biased systems.

From the comparison in Fig. 1, we can deduce an estimation of the interface oxide thickness. In fact, the Fe $L_{2,3}$ TEY spectra from the buried interface can be deconvoluted in the sum of the TEY spectra from semi-infinite Fe_3O_4 and Fe.[12,22] The relative weight R of the oxide contribution depends on the oxide thickness t and satisfies the following expression:[12,22]

$$R = e^{t(1/\lambda_e + 1/\lambda_x \cos\theta)} - 1. \tag{1}$$

In this expression, λ_x and λ_e are the x-ray absorption length and the secondary electron escape depth in the iron oxide layer, respectively, while θ is the angle between the surface normal and the light wave vector (for our data $\theta = 60°$). The presence of the NiO overlayer attenuates both signals from the iron substrate and from the interface oxide in the same way and does not modify the value of the ratio R. For the same reason, R is not affected by the possible presence of a nonuniform islanding structure in the NiO overlayer. Note also that possible saturation effects[22] are implicitly accounted for in the derivation of Eq. (1).[12,22] The photon-flux-normalized TEY absorption spectra from semi-infinite Fe and Fe_3O_4 can be found in Ref. 12. At the Fe $L_{2,3}$ maximum, the TEY intensity of the XAS spectrum from Fe_3O_4 is a factor 1.55 larger than that of the spectrum obtained from pure Fe.[12] From Fig. 1 we thus obtain that $R = 0.87 \pm 0.05$. Substituting in Eq. (1) the values $\lambda_e = (48 \pm 10)$ Å and $\lambda_x = (170 \pm 20)$ Å experimentally obtained for Fe_3O_4 in Ref. 23, we find an oxide thickness $t = (19 \pm 3)$ Å.

This result has been obtained assuming that the interface between the substrate and the iron oxide is sharp and flat. Although the good agreement in the comparison shown in Fig. 1 implies that the percentage of iron oxides other than Fe_3O_4 is very small, we cannot completely exclude the formation of different iron oxide species nor a gradient in the oxygen concentration in iron. Similarly, the presence of a Fe-Ni mixing at the interface, as in the case of Fe/NiO,[19] cannot be ruled out but, considering the results of Fig. 1, its spatial extension has to be much lower than the Fe_3O_4 film thickness. The aim of the thickness analysis reported above is, however, meant only to give an indication of the total amount of iron oxide that forms after NiO deposition. In this context, the morphology of the iron oxide has a little importance. In fact, the oxide thickness that we deduce with our analysis is such that $t \ll \lambda_x$ and $t \ll \lambda_e$. In this thickness range, $R \simeq t(1/\lambda_e + 1/\lambda_x \cos\theta)$. Since R is obtained from experimental spectra resulting from a spatial average on the sample due to the macroscopic x-ray beam size, R depends only on the *average* iron oxide thickness. Using the correct expression for R given in Eq. (1), we find that the average oxide thickness obtained from Fig. 1 does not cross the uncertainty bar given above for t, even assuming that the interface roughness could be as large as the entire iron oxide layer. It is interesting to notice that, in our NiO/Fe(100) interface, oxidation of the iron substrate extends on a larger depth with respect to Fe/NiO(100), where oxidation involves only the first two Fe atomic layers at contact with NiO.[12]

When Fe(001)-$p(1\times1)$O is formed, the oxygen atoms remain confined in the first atomic layer and protect the iron substrate from further oxidation.[13,14] The reactive deposition of NiO on the passivated Fe(001)-$p(1\times1)$O surface has the effect of promoting the substrate oxidation, resulting in the formation of a thick, oxygen-rich Fe_3O_4 layer. A similar behavior has recently been observed for the reactive deposition of NiO on Pd(001).[24] Ni is able to promote the reaction between O and Pd, which cannot be bulk oxidized at any temperature. This capacity of promoting Pd oxidation depends not only on the generic presence of Ni on the substrate surface, but also on the precise amount of the deposited metal.[24] This behavior has been correlated with the work-function lowering of the system, which is generally observed in the first stages of a metal/metal interface formation.[24] If the overlayer lowers the work function of the substrate, it makes it more reactive towards oxidation. This phenomenon is well known for alkali metals as oxidative promoters on transition metal substrates.[25] A similar lowering of the Fe(001)-$p(1\times1)$O work function upon Ni reactive deposition is thus expected to start the iron substrate oxidation, which is then energetically favored by the lower electronegativity of Fe compared to Ni. Another possible mechanism could be that atomic oxygen is produced as a consequence of the chemical reaction between a Ni atom and an O_2 molecule, resulting in the formation of NiO. Fe oxidation would take place because atomic oxygen is more mobile and reactive than molecular oxygen.

We have also investigated the effects of annealing on the buried interface obtained after reactive NiO deposition. The knowledge of the interface behavior upon annealing is particularly important in the physics of exchange biased systems. Let us recall that annealing above the AFM Néel temperature is a typical procedure used for obtaining exchange bias FM/AFM devices. The bottom part of Fig. 2 shows the Fe $L_{2,3}$ XAS spectra of the Fe(001)-$p(1\times1)$O substrate, of room temperature grown NiO/Fe(001), and of NiO/Fe(001) annealed at 350 and 450 °C for a few seconds. Although a sizeable contribution from the metal iron substrate is present

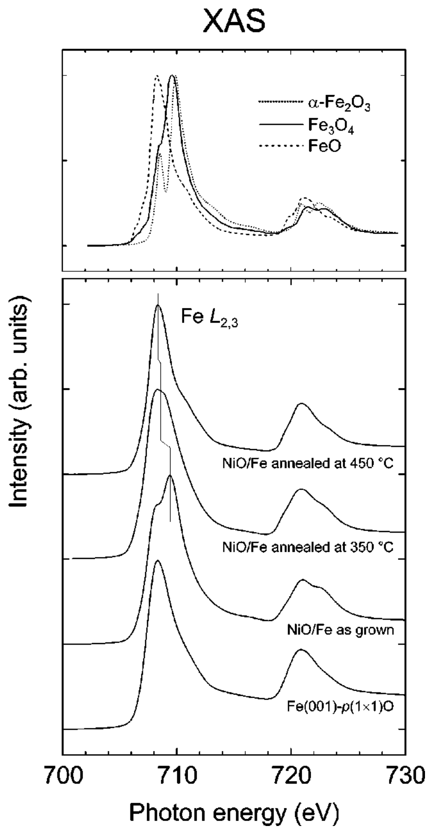

FIG. 2. Bottom: comparison between the Fe $L_{2,3}$ XAS spectra obtained in the TEY mode from Fe(001)-$p(1\times1)$O and 20 ML NiO/Fe(001), as grown and after annealing. Top: absolute absorption spectra at the Fe $L_{2,3}$ edge from α-Fe_2O_3, Fe_3O_4, and FeO (from Ref. 12).

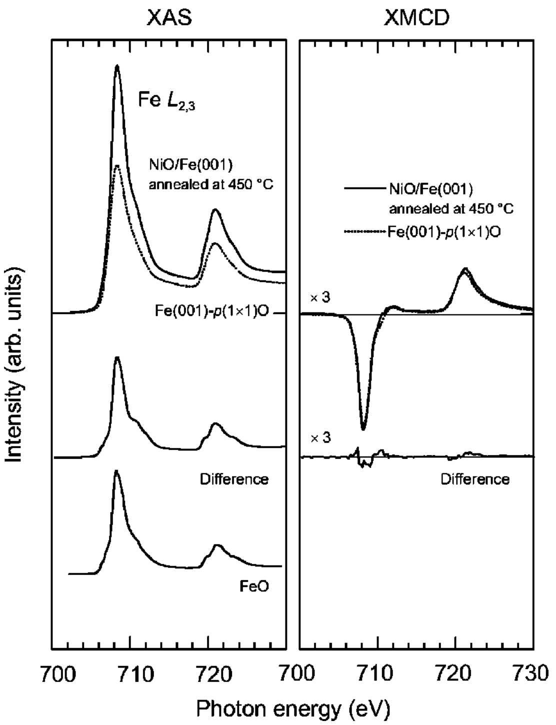

FIG. 3. Comparison between the Fe $L_{2,3}$ XAS (left) and XMCD (right) spectra from annealed 20 ML NiO/Fe(001) and Fe(001)-$p(1\times1)$O. After normalization, the spectra obtained on Fe(001)-$p(1\times1)$O have been multiplied by a factor equal to 0.6. The difference XAS spectrum is compared to the FeO XAS (from Ref. 12).

in the spectra, it is quite apparent that the centroid of the Fe $L_{2,3}$ edge XAS shifts towards lower photon energies as the annealing temperature of NiO/Fe(001) is increased. From the top part of Fig. 2, displaying the Fe $L_{2,3}$ edge absolute absorption spectra of Fe_3O_4, α-Fe_2O_3, and FeO (Ref. 12), it can be seen that such a shift is associated with the iron oxidation state. In particular, the shift shown by the XAS in Fig. 2 indicates a reduction of the oxide: the iron valence is Fe^{2+} in FeO and Fe^{3+} in Fe_2O_3, while Fe_3O_4 is characterized, as mentioned above, by the simultaneous presence of Fe^{2+} and Fe^{3+} sites.

Similar to Fig. 1, in Fig. 3 the metal Fe contribution is subtracted from the NiO/Fe(001) sample annealed at 450 °C. The XAS difference spectrum is very similar to the one measured on bulk FeO (from Ref. 12), while the XMCD difference spectrum vanishes as expected for an antiferromagnetic compound such as FeO. The same procedure that has been applied to estimate the Fe_3O_4 thickness from the data presented in Fig. 1 can be applied to the XAS spectra in Fig. 3. We shall assume that $\lambda_e = 30$ Å as in Ref. 12. We could not find in the literature the experimental λ_x value in FeO. However, at the Fe $L_{2,3}$ edge, λ_x is basically determined by the density ρ_{Fe} of iron atoms in the solid, since a core hole localized on a Fe atom is produced in the absorption process of an x-ray photon at threshold. We thus expect that $1/\lambda_x$ scales as ρ_{Fe}, so that the $1/\lambda_x$ value for FeO can be reasonably derived from the one for Fe_3O_4 and from the respective densities. FeO has a density of 6 g/cm^3 and the Fe atoms represent 77% of the total mass ($\rho_{Fe} = 4.67$ g/cm^3). In Fe_3O_4, which has a density equal to 5.17 g/cm^3, 72% of the mass is constituted of Fe, giving $\rho_{Fe} = 3.74$ g/cm^3. We then derive that $\lambda_x(\mathrm{FeO}) \simeq 0.8\ \lambda_x(\mathrm{Fe_3O_4}) = 136$ Å. Reference TEY spectra from thick Fe and FeO can be found in Ref. 12. From their relative intensities and from Fig. 3, we obtain $R = 0.48 \pm 0.05$. Assuming a 50% uncertainty in the determination of both λ_e and λ_x,[26] we can deduce a FeO thickness $t = (8 \pm 3)$ Å. The oxide thickness is thus unequivocally reduced upon annealing. Note that, since the densities of O atoms in FeO and Fe_3O_4 are similar (1.45 and 1.38 g/cm^3, respectively), this result leads to the conclusion that, upon annealing, the total amount of oxygen in the iron oxide is drastically decreased. We believe that this is due to oxygen desorption from the oxide layers during annealing. The surfaces of 3*d* transition oxides are in fact known to be unstable and to desorb oxygen when heated. This has been confirmed also in thin NiO film on a Ni metal substrate, where NiO starts decomposing at a temperature of 550 K.[27]

Because of the instability of the NiO film at high temperature, the annealing not only affects the oxidation state of the substrate, but is expected to have a dramatic effect on the NiO overlayer as well. Duò *et al.* demonstrated that in these films, upon annealing, a Ni-Fe substitution occurs, leading to the formation of iron oxide at the surface.[11] These results, obtained from photoemission data, are confirmed on a larger

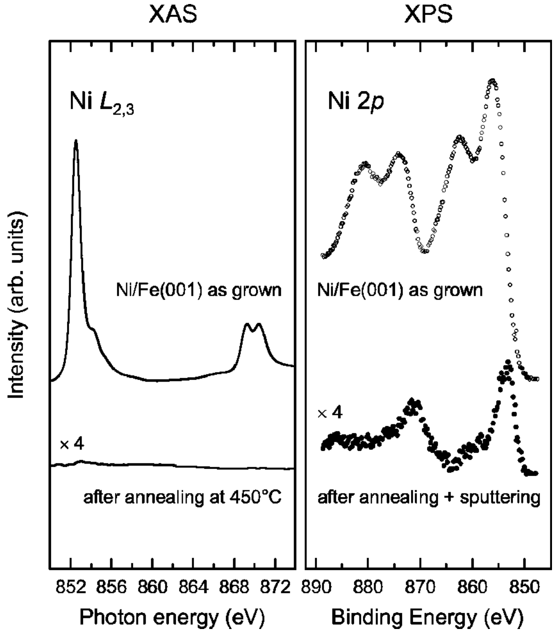

FIG. 4. Comparison between the TEY Ni $L_{2,3}$ XAS spectra from 20 ML NiO/Fe(001) before and after annealing at 450 °C. The spectra have been normalized to the photon flux. In the inset: Ni 2p XPS spectrum after annealing followed by sputtering.

probing depth scale by the x-ray absorption spectra reported in Fig. 4, showing the Ni $L_{2,3}$ edge XAS of NiO/Fe(001) before and after annealing. It is quite obvious that the Ni signal is completely lost after annealing. To demonstrate that Ni migrates into the substrate, in the inset of Fig. 4 we show the x-ray photoemission spectrum (XPS) of the Ni 2p core levels after the annealed sample had been sputtered to remove the iron oxide layer. The statistics is poor since Ni is very diluted in the Fe substrate. The Ni 2p XPS shows a line shape typical of metal Ni, indicating that both the iron oxide layer and the nickel diffusing into the substrate are reduced upon annealing. No trace of oxygen is detected after the removal of the FeO layer, reinforcing the conclusion that oxygen dilution into the iron substrate during annealing is negligible.

IV. SUMMARY AND CONCLUSIONS

We have reported a XAS and XMCD study of the NiO/Fe(001) interface, obtained by reactive Ni deposition in O_2 atmosphere onto the passivated Fe(001)-$p(1\times1)$O surface. This reactive deposition promotes Fe oxidation, leading to the formation of a buried layer of Fe_3O_4, which couples ferromagnetically to the iron substrate. The buried Fe_3O_4 magnetization is reduced by a factor of 2 with respect to bulk Fe_3O_4. When 20 ML NiO are grown on Fe(001)-$p(1\times1)$O, a 19 Å thick Fe_3O_4 layer is produced at the interface. This result is considerably different from the case of the inverted Fe/NiO(001) interface where formation of antiferromagnetic FeO takes place. This means that, although the involved elements are the same in both AFM/FM and FM/AFM systems, the chemical reactions occurring at the interface give different products. The reason for this is intrinsically related to the growth process itself, during which the amount of oxygen available is largely different for the two cases. This effect has important consequences in AFM/FM devices in which both types of interfaces are present, and should not be neglected in models describing their transport and magnetic properties.

A sample annealing following the growth of the NiO/Fe interface is found to completely destroy the NiO overlayer. The nickel atoms completely dissolve into the substrate and the oxidation state of the resulting iron surface is very similar to FeO, representing a reduction of the buried oxide layer obtained before annealing.

---

*Electronic address: marco.finazzi@fisi.polimi.it

[1] W. H. Meiklejohn and C. P. Bean, Phys. Rev. **102**, 1413 (1956); **102**, 904 (1957).
[2] S.-H. Tsai, D. P. Landau, and T. C. Schulthess, J. Appl. Phys. **93**, 8612 (2003).
[3] M. Finazzi, Phys. Rev. B **69**, 064405 (2004).
[4] U. Nowak, K. D. Usadel, J. Keller, P. Miltényi, B. Beschoten, and G. Güntherodt, Phys. Rev. B **66**, 014430 (2002); U. Nowak, A. Misra, and K. D. Usadel, J. Magn. Magn. Mater. **240**, 243 (2002).
[5] H. Ohldag, T. J. Regan, J. Stöhr, A. Scholl, F. Nolting, J. Lüning, C. Stamm, S. Anders, and R. L. White, Phys. Rev. Lett. **87**, 247201 (2001).
[6] J. Camarero, Y. Pennec, J. Vogel, S. Pizzini, M. Cartier, F. Fettar, F. Ernult, A. Tagliaferri, N. B. Brookes, and B. Dieny, Phys. Rev. B **67**, 020413(R) (2003).
[7] H. Matsuyama, C. Haginoya, and K. Koike, Phys. Rev. Lett. **85**, 646 (2000).
[8] W. Zhu, L. Seve, R. Sears, B. Sinkovic, and S. S. P. Parkin, Phys. Rev. Lett. **86**, 5389 (2001).
[9] H. Ohldag, A. Scholl, F. Nolting, S. Anders, F. U. Hillebrecht, and J. Stöhr, Phys. Rev. Lett. **86**, 2878 (2001).
[10] M. Finazzi, M. Portalupi, A. Brambilla, L. Duò, G. Ghiringhelli, F. Parmigiani, M. Zacchigna, M. Zangrando, and F. Ciccacci, Phys. Rev. B **69**, 014410 (2004).
[11] L. Duò, M. Portalupi, M. Marcon, R. Bertacco, and F. Ciccacci, Surf. Sci. **518**, 234 (2002).
[12] T. J. Regan, H. Ohldag, C. Stamm, F. Nolting, J. Lüning, J. Stöhr, and R. L. White, Phys. Rev. B **64**, 214422 (2001).
[13] R. Bertacco and F. Ciccacci, Phys. Rev. B **59**, 4207 (1999).
[14] J. B. Benziger and R. Madix, J. Electron Spectrosc. Relat. Phenom. **20**, 281 (1980).
[15] M. Zangrando, M. Finazzi, G. Paolucci, G. Comelli, B. Diviacco, R. P. Walker, D. Cocco, and F. Parmigiani, Rev. Sci. Instrum. **72**, 1313 (2001).
[16] V. Chakarian, Y. U. Idzerda, and C. T. Chen, Phys. Rev. B **57**, 5312 (1998).
[17] H.-J. Kim, J.-H. Park, and E. Vescovo, Phys. Rev. B **61**, 15 284

(2000).

[18] F. Sette, C. T. Chen, Y. Ma, S. Modesti, and N. V. Smith, in *X-ray Absorption Fine Structure*, edited by S. S. Hasnain (Ellis Horwood, New York, 1991) p. 96.

[19] P. Luches, M. Liberati, and S. Valeri, Surf. Sci. **532/535**, 409 (2003); S. Benedetti, P. Luches, M. Liberati, and S. Valeri, *ibid.* **572**, L348 (2004).

[20] F. Ciccacci, L. Duò, and E. Puppin, Surf. Sci. **269/270**, 533 (1992).

[21] P. Kuiper, B. G. Searle, L.-C. Duda, R. M. Wolf, P. J. van der Zaag, J. Electron Spectrosc. Relat. Phenom. **86**, 107 (1997).

[22] R. Nakajima, J. Stöhr, and Y. U. Idzerda, Phys. Rev. B **59**, 6421 (1999).

[23] S. Gota, M. Gautier-Soyer, and M. Sacchi, Phys. Rev. B **62**, 4187 (2000).

[24] M. Sambi, R. Resolo, G. A. Rizzi, M. Petukhov, G. Granozzi, Surf. Sci. **537**, 36 (2003).

[25] R. D. Diehl, R. McGrath, J. Phys.: Condens. Matter **9**, 951 (1997).

[26] The large uncertainty associated with λ_e in FeO may be justified since the value reported in Ref. 12 seems to lack a firm experimental basis. By admitting a 50% uncertainty we implicitly assume that λ_e in FeO could be as large as in Fe_3O_4, in which $\lambda_e \simeq 48$ Å (see Ref. 23).

[27] N. Kitakatsu, V. Maurice, and P. Marcus, Surf. Sci. **411**, 215 (1998).